2004-01-2147

Application of a Finite Element-Based Human Arm Model for Airbag Interaction Analysis

Joseph J. Mihm and Stephen A. Ridella
TRW Automotive

Lex Van Rooij and Jack van Hoof
TNO Automotive

ABSTRACT

Interaction of the human arm and deploying airbag has been studied in the laboratory using post mortem human subjects (PMHS). These studies have shown how arm position on the steering wheel and proximity to the airbag prior to deployment can influence the risk of forearm bone fractures. Most of these studies used older driver airbag modules that have been supplanted by advanced airbag technology. In addition, new numerical human body models have been developed to complement, and possibly replace, the human testing needed to evaluate new airbag technology. The objective of this study is to use a finite element-based numerical (MADYMO) model, representing the human arm, to evaluate the effects of advanced driver airbag parameters on the injury potential to the bones of the forearm. The paper shows how the model is correlated to Average Distal Forearm Speed (ADFS) and arm kinematics from two PMHS tests. The PMHS testing employed different offsets (0 and 25mm) between the airbag and forearm in a driving position, using the two arms of the same human subject. The model is then exercised to determine predictive ability for forearm fracture seen with the 0mm offset test, but not seen with the 25mm offset. The model accurately predicts fracture in the 0mm offset test, and no fracture in the 25mm offset test using a ADFS criterion of 10.5 m/s. Model elements in the ulna that rapidly exceed an arbitrary 1% effective strain criteria correspond to fracture locations on the ulna of the 0mm offset PMHS test. The model is then exercised to predict fracture using the ADFS criterion for multiple inflator outputs. The paper also discusses issues and recommendations for human model parameters to further increase the robustness of the model.

INTRODUCTION

Airbags have been introduced into passenger vehicles for several decades, providing crash protection in both frontal and side impacts. These devices have significantly reduced traumatic injuries caused by crashes, however, some evidence exists that the devices themselves may be contributing to some non-fatal injuries to occupants such as bone fractures to the extremities, specifically the forearm. In a detailed field study [Huelke 1997], 540 crashes were investigated where driver airbags deployed. A total of 34% of the drivers sustained Abbreviated Injury Scale (AIS) 1 upper extremity injuries, with an additional 3% that sustained AIS 2+ injury. Of the 18 drivers that sustained AIS 2+ upper extremity injuries, six sustained the injury from direct contact with a deploying airbag. In addition, NASS CDS (National Automotive Sampling System Crashworthiness Data System) shows an increase from 1.1% to 4.4% in the occurrence of AIS 2+ upper extremity injuries that were a result of an airbag deployment [Kuppa 1997].

Attempts to analyze the interaction between a deploying airbag and a human arm have consisted primarily of cadaveric impact experiments. Preliminary injury criteria relating to the Average Distal Forearm Speed (ADFS) has been developed using this technique (Hardy 2002). An ADFS value of 10.5 m/s was established corresponding to a fifty-percent probability of forearm fracture at AIS≥2 levels. This study also concluded that fracture incidence and severity were related to the test subject's physical state (bone mass, mineral content) as well as the airbag's aggressivity and the subject's proximity to the airbag.

Issues with testing Post Mortem Human Subjects (PMHS) for these types of interaction studies have prompted the need for reliable analytical models to be used. Reliable models are being developed [van Rooij 2003] which can allow us to study specific human-to-airbag interactions. The goal of this study is to use the MADYMO Finite Element Model (FEM) of the human arm (developed by TNO within the European HUman MOdel for Safety project (HUMOS)[Robin 2001]) to evaluate forearm interactions with a simulated deploying airbag and cover. It evaluates the model correlation to

previous PMHS studies (Hardy 1997), focusing on arm kinematics and velocities. Furthermore, the model is used to study the relationship between forearm bone material stresses, and strains, to airbag parameters such as ballistic output. The study will also begin to evaluate the models ability to predict fracture.

METHODS

MODEL CREATION and CORRELATION TO PMHS TESTING - The model used for this study consisted of the MADYMO 50th percentile global human model coupled with the 50th percentile male FE arm model, version 6.1. To study the effects of airbag interaction, this model was correlated to two full-scale cadaveric tests from a series performed by Hardy, et al. [Hardy 1997]. Test numbers used were T9619 and T9620. The comparison between the PMHS subjects and the model are shown in Table 1.

To more closely approximate the tests, the following changes were made to the model:

- Two accelerometer bodies with a mass of 24 grams each were created and attached to the proximal and distal radius to simulate the accelerometer blocks used in the tests. Linear velocity output from these was used to compare to integrated cadaver accelerometer data.
- Arm mass was lowered from 3.90 to 2.96 kg by reducing the density of the muscle, fat, flesh, and hand as follows
    - Hand density reduced from 6000 to 2363 kg/m3
    - Skin, muscle, fat, flesh density reduced from 1000 to 694 kg/m3

A finite element model of the deployment door was created from CAD data using shell elements. A tear seam was simulated using spotwelds at the tear seam opening. A FEM model of the driver bag was used that duplicated the folded bag used in the tested modules. A constant-pressure simulation was used for the mass flow with a circular jet directing the gas into the bag. The mass flow was generated using a constant-temperature method from a 28.3 liter closed tank ballistic test. The inflator used for model correlation to cadaver testing had a pressure-time profile (of nitrogen gas) of 424 kPa peak x 17 kPa/ms slope. The mass flow and pressure-time profiles are shown in Figure 1.

Cadaver test subjects were selected based on their approximation to the 50th percentile male human model. The cadavers were seated in a rigid seat (22 deg. seatback angle) in a simulated driving position. The airbag module was mounted in a steering wheel with a 45 deg. column angle. The cadaver was offset from the center of the wheel to allow full motion of the arm. The arm was placed on top of the airbag module perpendicular to the airbag (horizontal) tear seam. In a series of 2 tests, one arm was spaced at 0mm from the module, which induced a fracture, and the other arm was spaced at 25mm, which did not induce fracture. This would allow the model's ability to predict fracture using the same human subject.

Table 1: Parameters of Test and Simulation

Test	Hardy T9619	Hardy T9620	Model
Gender	Male		Male
Age	77		
Stature (cm)	178		173
Mass (kg)	86		80
Arm	Right	Left	Left
Arm Mass (kg)	2.72	2.68	2.96
Inflator	424x17 (28.3l tank)	424x17 (28.3l tank)	424x17 (28.3l tank)
Arm/Airbag Spacing (mm)	0	25	0/25
Column Angle (deg)	45	45	45

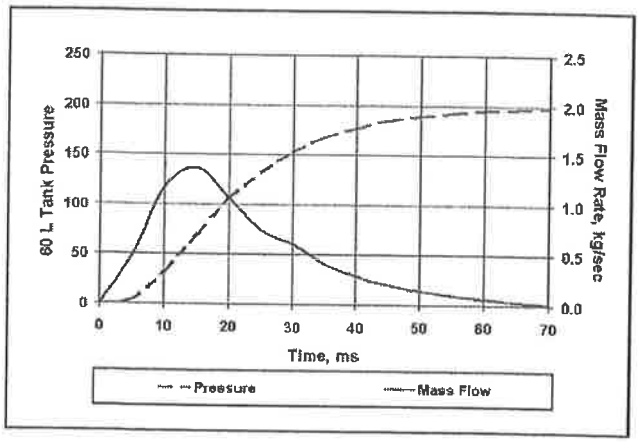

Figure 1. Ballistic properties of "424x17" inflator used in cadaveric tests T9619 and T9620 [Hardy 1977]. (Pressure-time profile estimated from 28.3 liter tank data).

Radial velocity correlation, 0mm offset – Using accelerometer bodies weighing 24 grams and attached to the radius, the model was correlated to the tests for

linear velocity. In the 0 mm offset case (forearm placed directly on deployment door), using a common start time of the onset of bag pressure, a reasonable correlation for both distal (Figure 2a.) and proximal (Figure 2b.) velocities is achieved. In the time frame of interest (0-15 ms) when the door and airbag have the highest degree of interaction, the distal velocity correlation is very close, even demonstrating a bi-modal profile. After 15ms, the model velocities are significantly lower due to less "flinging" of the arm that was observed in the test. The proximal velocities have similar velocity traces, although the peak velocities are lower. A comparison of the kinematics of the model vs. test is shown in sequence in Figures 4a. – 7a., and 4b.-7b..

Radial velocity correlation, 25mm offset - Using the same accelerometer models as the 0mm condition, the arm of the model was placed approximately 25mm off of the deployment door and used to compare distal and proximal radial velocities to test T9620 (Figures 3a., 3b.) The model shows good correlation, with similar trends seen with the 0mm offset condition.

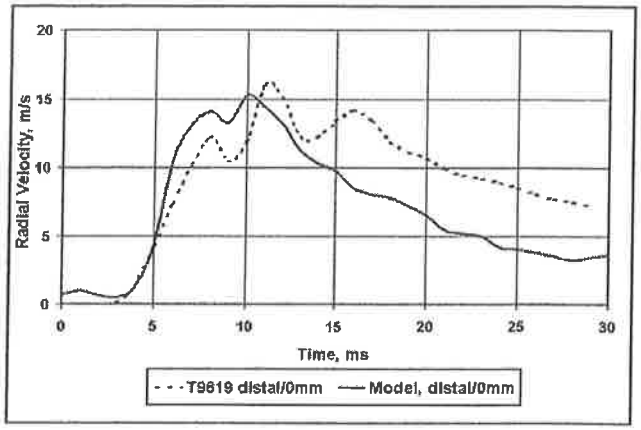

Figure 2a. Distal radial velocity correlation to PMHS testing with 0mm offset of arm to module.

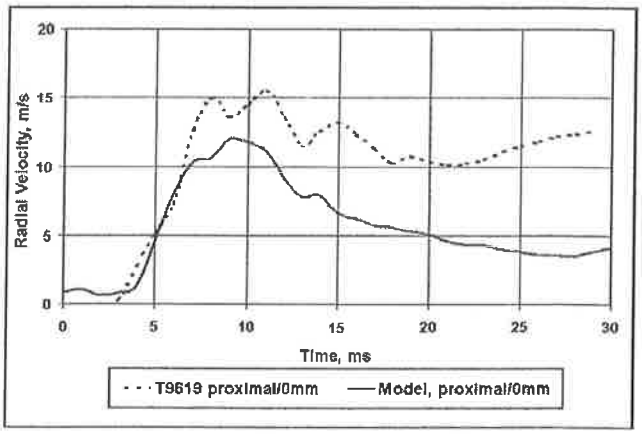

Figure 2b. Proximal radial velocity correlation to PMHS testing with 0mm offset of arm to module.

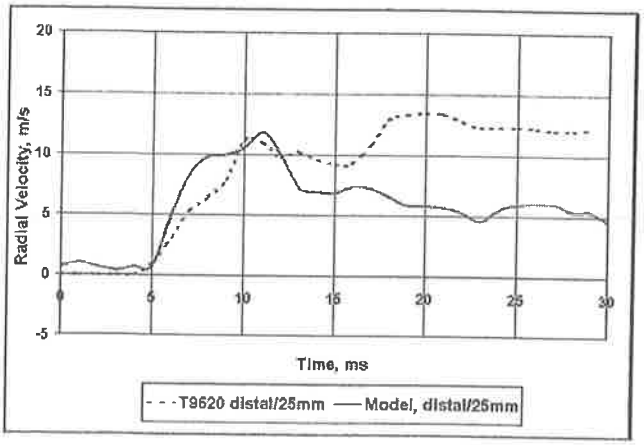

Figure 3a. Distal radial velocity correlation to PMHS testing with 25mm offset of arm to module.

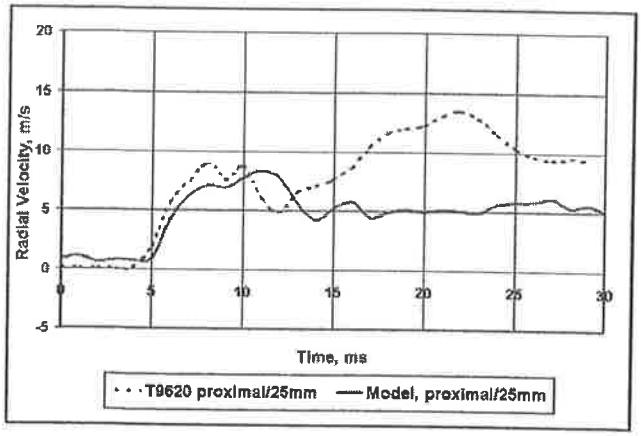

Figure 3b. Proximal radial velocity correlation to PMHS testing with 25mm offset of arm to module.

Using the model to predict fracture – In Hardy et al. [Hardy 1997, 2002], an Average Distal Forearm Speed (ADFS) of 10.5 m/s was established to correspond to a fifty percent probability of forearm fracture at AIS ≥2 levels. Using this criterion, the model velocity exceeds the criterion indicating a high probability of fracture of the forearm (Table 2.)

Table 2. Injury measures for Test vs. and Model

	0mm Offset		25mm Offset	
Injury Measure	**T9616**	**Model**	**T9620**	**Model**
Ave. Distal Forearm Speed (m/s)	12.6	12.9	9.4	7.7
Peak Distal Forearm Speed (m/s)	17.1	15.7	11.4	11.9

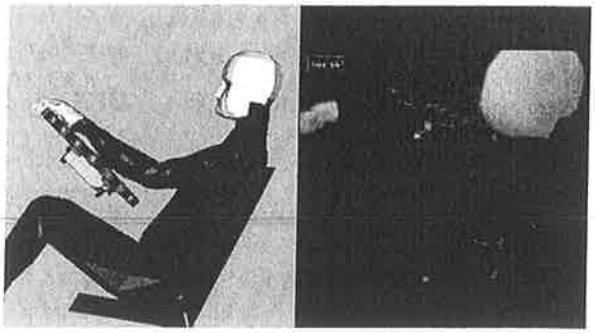

Figure 4a. Test vs. Model set up for 0mm offset condition (T9619) at time = 0ms. (Side view)

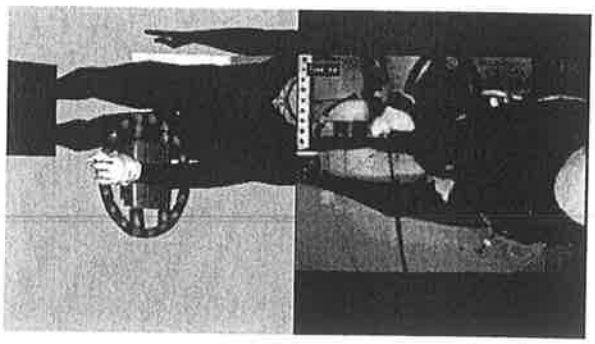

Figure 4b. Test vs. Model set up for 0mm offset condition (T9619) at time = 0ms. (Top view)

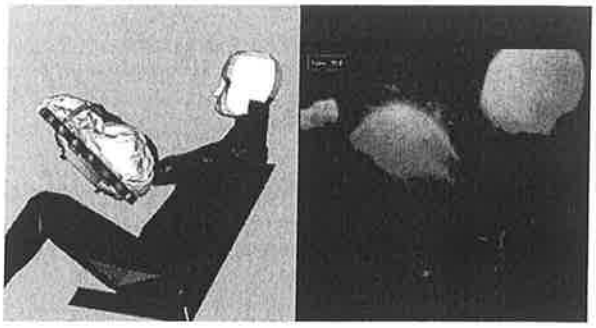

Figure 5a. Test vs. Model set up for 0mm offset condition (T9619) at time = 15ms. (Side view)

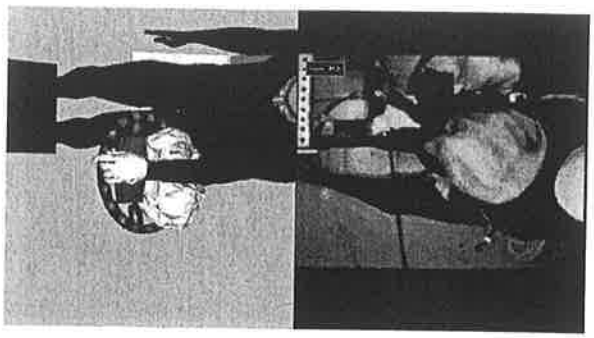

Figure 5b. Test vs. Model set up for 0mm offset condition (T9619) at time = 15ms. (Top view)

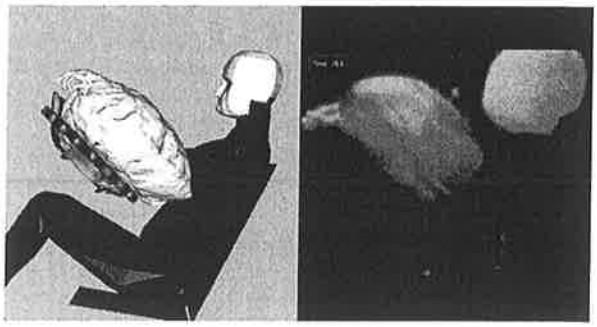

Figure 6a. Test vs. Model set up for 0mm offset condition (T9619) at time = 20ms. (Side view)

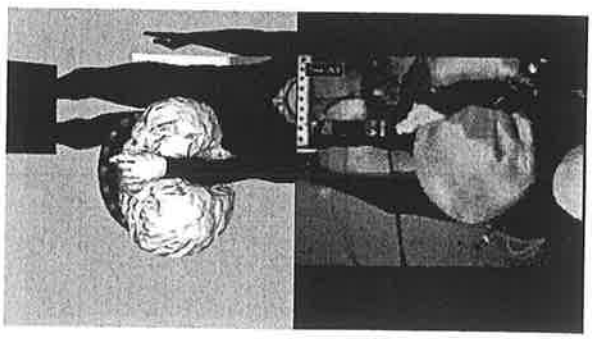

Figure 6b. Test vs. Model set up for 0mm offset condition (T9619) at time = 20ms. (Top view)

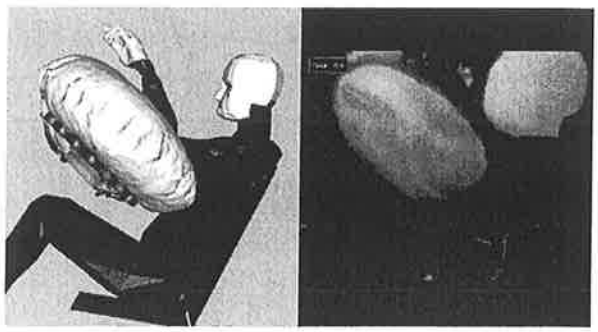

Figure 7a. Test vs. Model set up for 0mm offset condition (T9619) at time = 25ms. (Side view)

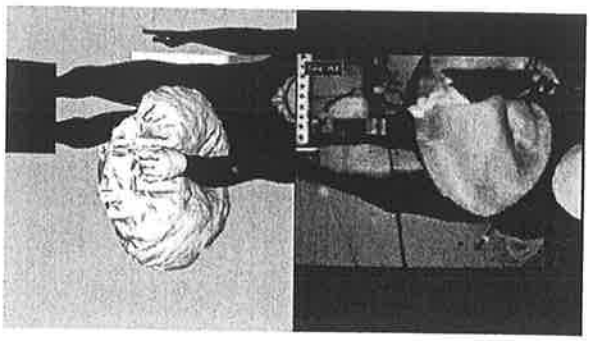

Figure 7b. Test vs. Model set up for 0mm offset condition (T9619) at time = 25ms. (Top view)

Using strain to predict fracture – An elasto-plastic material model was chosen for the finite element bone in the model. The bone "fails" at its yield point, but is then free to strain more. In the experiments, when bone failure occurs the measured strain becomes zero, and the properties of the arm change due to the fracture. For this study, an arbitrary value for effective plastic strain of 1.0% is used as a criteria for when bone failure will likely occur. Experimental wet bone data [Rooij 2003, Fung 1981] for long bones of a 20-39 year old human (femur, tibia, humerus, radius) have ultimate elongations that range from 1.41 – 1.50%.

Review of strain outputs from the 0mm offset model revealed four ulnar elements that demonstrated a significantly higher strain rate than the majority of the elements found in the long (non-joint) portions of the bones. These elements are shown darkened in Figure 8., as indicated by the arrows. The elements of high strain found on the ulna (3200, 3101, 3057, 3266) are grouped in an area that corresponds to a distance of approximately 119mm to 135mm from the styloid. This corresponds very well with the necropsy report from the cadaver (Figure 9.), test T9619, which had a diaphyseal dorsal wedge fracture of the ulna starting at 90mm, centered at 121mm, and ending at 148mm from the styloid [Hardy 1997]. Other injuries included a simple, oblique, diaphyseal fracture of the ulna starting at 169mm and ending at 177mm from the styloid. 9[Hardy 1977].

From Figure 10., we see that the four ulnar elements reach or exceed a 1.0% strain level before four similar radial elements do, so ulnar fracture could be predicted before radial fracture based on the criteria. The ulnar elements, as a group, also "plateau" out close to the peak stress of 100Mpa, which the radial elements do not.

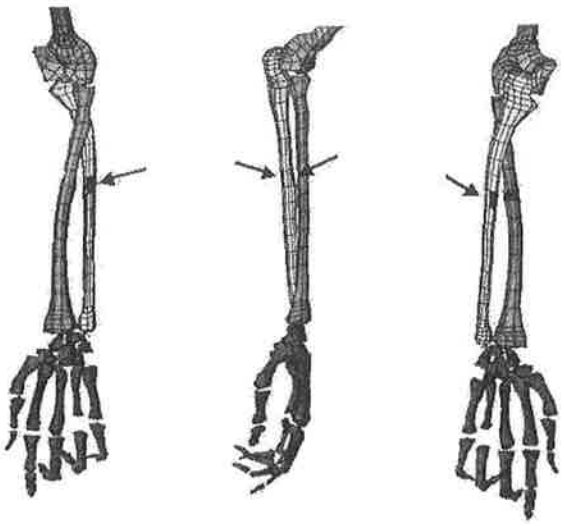

Figure 8. Ulnar elements experiencing high strain rates in 0mm offset model. (Note: Model is left arm, fracture occurred in right arm of test T9619).

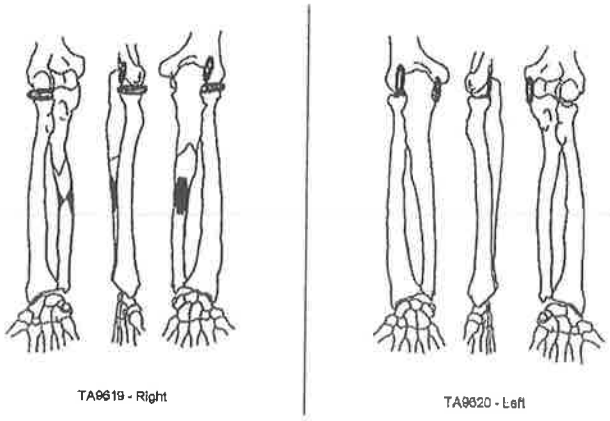

Figure 9. Necropsy results from 0mm offset test T9619 showing ulnar fractures.

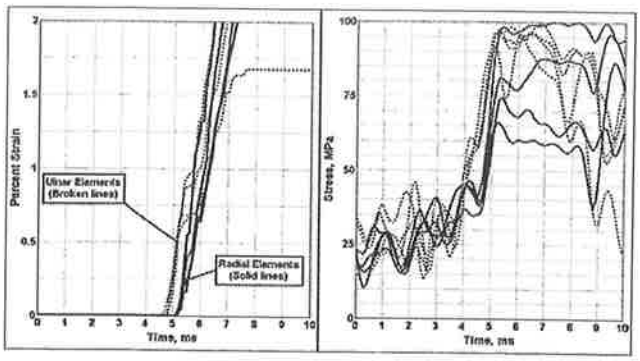

Figure 10. Strain and Von Mises stress profiles of highest strained ulnar and radial elements found in 0mm offset simulation.

APPLICATION – An application for a human body model presents itself in the study of airbag interactions with the arm and the influence of airbag parameters on fracture potential. Using the model correlated to PMHS test as described earlier, a series of inflators with a wide range of ballistic outputs (Figures 11, 12) were evaluated. (Note- the inflator used in the correlation to test T9619, -20, corresponds to inflator "C"). The range of inflators was selected to represent what could possibly be encountered in the field, from high, pre-depowered systems, to low, single-stage only "smart" systems being developed. In addition, the influence on proximity to the airbag can be observed.

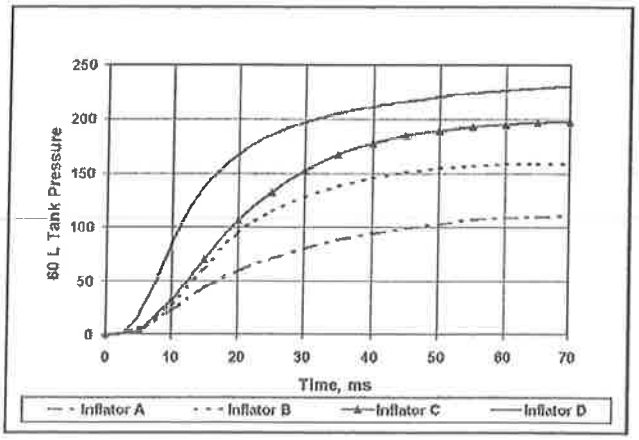

Figure 11. Inflator pressure-time profiles used for inflator aggressivity modeling.

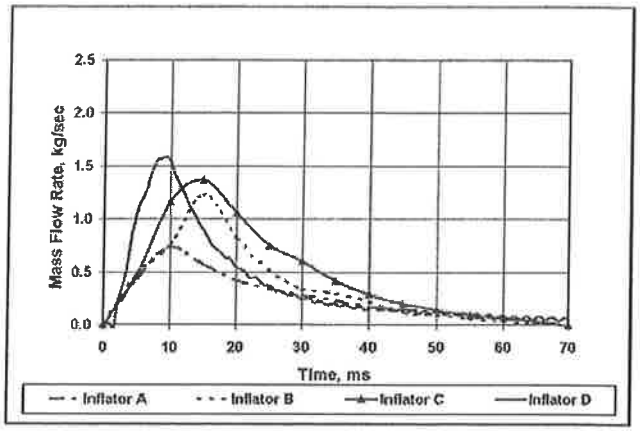

Figure 12. Inflator mass flow profiles used for inflator aggressivity modeling.

Results of distal forearm speeds are shown in Figures 13 (0mm offset) and 14 (25mm offset). Table 3 summarizes the ADFS and PDFS (Peak) for the models studied. (Ref. Hardy 2002, p.13, for ADFS calculation).

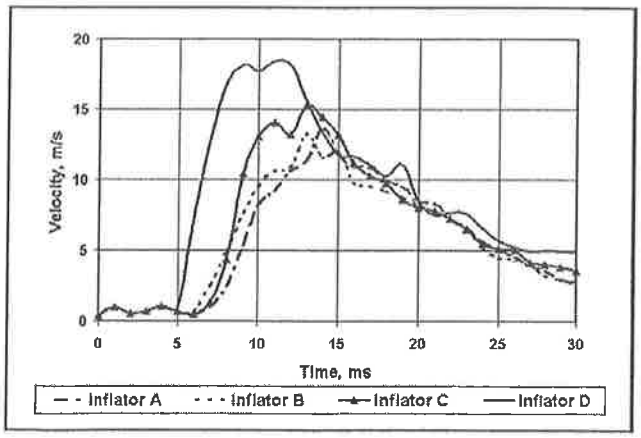

Figure 13. Distal radial velocities at 0mm offset of arm to airbag module (data from model time zero).

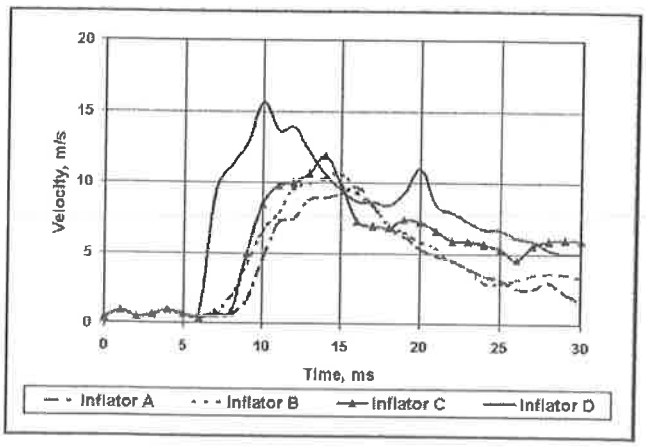

Figure 14. Distal radial velocities at 25mm offset of arm to airbag module (data from model time zero).

Table 3. Forearm speeds for various stand-offs and ballistic outputs.

Stand-off	0mm		25mm	
Inflator	PDFS (m/s)	ADFS (m/s)	PDFS (m/s)	ADFS (m/s)
A	13.9	8.6	9.9	4.3
B	13.3	9.5	11.1	6.5
C	15.7	12.9	11.9	7.9
D	19.2	16.9	15.7	12.9

DISCUSSION

In the attempt to correlate the human body model to cadaveric tests, two main issues were encountered. First, the mass of the arm had to be adjusted by changing tissue properties to more closely match those of the subjects being tested. Secondly, the stability of the model has proven very sensitive to the proper establishment of FEM-to-FEM contact parameters. When these were finally developed to a satisfactory point, satisfactory arm kinematics were obtained with a corresponding good relationship to distal forearm velocities, particularly in the time frame when the deployment door and airbag are in direct contact with the arm. Arm kinematics and velocity correlation degrade later in the event as the arm is flung from the module. This could be due to shoulder joint kinematics or the change in arm properties when fracture occurs in the human subjects.

Using the ADFS criteria developed by Hardy, et al., the onset of forearm fracture (T9619) may be predicted from the model. It can also be used to analyze the effect of various inflator outputs on potential injury to the arm. If the data from Table 3 is charted as shown in Figure 15, some interesting trends are observed. For example inflators B and C may have similar ballistic pressure-time slopes (Figure 11), but inflator C has a significantly higher ADFS (at 0mm stand-off), pushing over the preliminary level of 10.5 m/s established by Hardy, et al.. We also see a significant drop off in ADFS as the arm moves off of the module, which keeps all but the very high-output D inflator under the preliminary criteria.

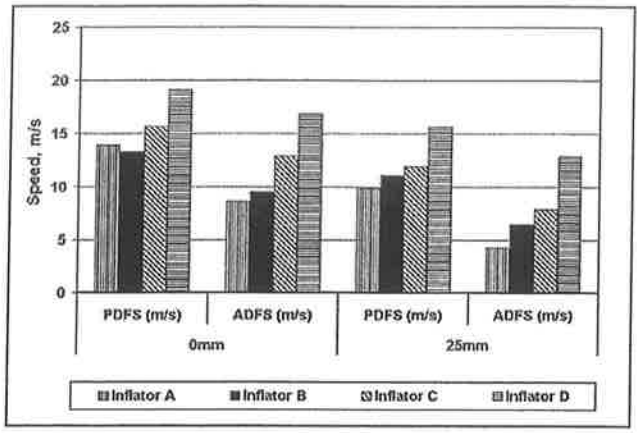

Figure 15. Using the human arm model to study the influence of ballistic output and module stand-off.

There are still issues with using the model to predict bone fracture. If we use the ADFS criteria alone, it does not predict where the fracture might occur. If we use bone strain to predict fracture, the level of 1% is arbitrary, and failure strains can vary with bone location and age [Fung 1981]. This is also true for the ultimate tensile strength of the bone. The model currently uses a value of 100Mpa, although Fung et al. shows a range of 152+/- 1.4 Mpa for the radius for a subject 20-39 years of age. The model did correctly locate where fracture was likely to occur by identifying elements with locally high strain rates, although it appears that prediction of the fracture is more closely related to where the ultimate tensile stress of the bone is locally exceeded.

Qualitatively, we can use Von Mises stress contours as shown in Figures 16 and 17 to determine the onset of localized bone stress that exceeds a given value. In this graphic, the first areas of forearm to begin to approach or exceed 100Mpa are located at the proximal ulna, which is where the fracture occurred. According to crack detectors used on T9619, the fracture occurred at 8.7 ms [Hardy 1997], although the model predicts the high stress levels achieved between 5 and 6 milliseconds.

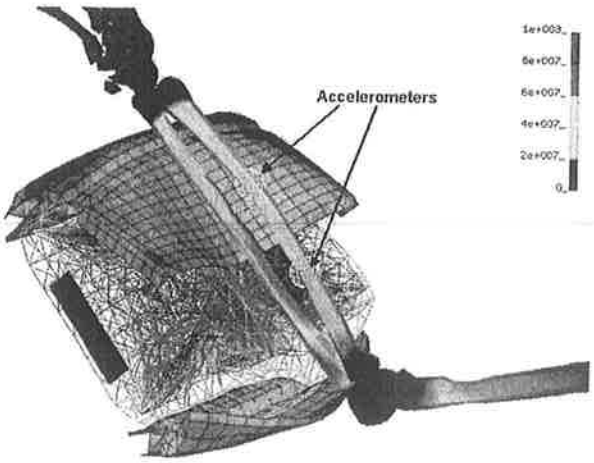

Figure 16. Von Mises bone stress at t=5ms for simulation of T9619.

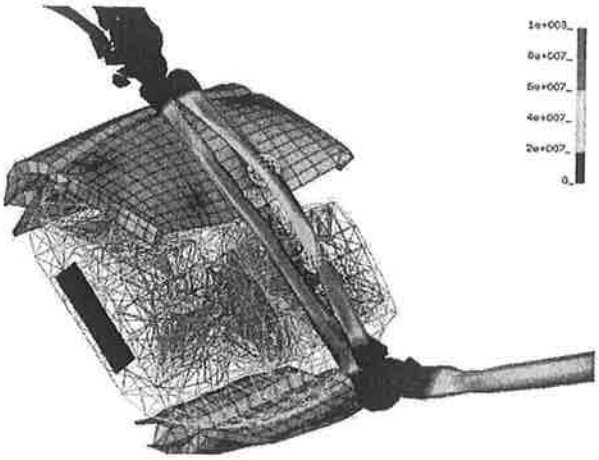

Figure 17. Von Mises bone stress at t=6ms for simulation of T9619.

CONCLUSION

Human body models have the potential to replace Post Mortem Human Subjects when analyzing the interaction of airbags with human subjects. This study showed that a current human arm model could correlate well with a PMHS whose forearm was subjected to direct interaction with a deploying airbag with a tear-seamed deployment door. The model predicted the Average Distal Forearm Speed, which in turn successfully predicted the fracture that occurred in the PMHS. In addition, the model has shown the potential to further predict both the potential for as well as the *location* of a fracture using strain and stress criteria in the bone elements. Further investigation is needed to determine the robustness of the model, as well as its predictive capabilities.

ACKNOWLEDGMENTS

The authors acknowledge the early modeling work done by Suk Jae Ham.

REFERENCES

1. Fung, Y. C., (1981) Biomechanics, Mechanical Properties of Living Tissues, Springer-Verlag Pub.
2. Hardy, W. N., Schneider, L. W., Reed, M. P., and Ricci, L. L. (1997) Biomechanical Investigation of Airbag-induced Forearm Fractures and Airbag Aggressivity. Proc. 45th Stapp Car Crash Conference, Society of Automotive Engineers, Warrendale, PA.
3. Hardy, W. N., and Schneider, L. W., (2002) Identification of Injury Mechanisms Resulting in Injuries to the Upper Extremities in Frontal Crashes, The University of Michigan Transportation Research Institute, Ann Arbor, MI.
4. Huelke, D. F., Gilbert, R., and Schneider, L. W., (1997) Upper–extremity Injuries from Steering Wheel Air Bag Deployments. SAE International Congress, SAE 970493
5. Kuppa, S. M., Olson, M. B., Yeiser, C. W., Taylor, L. M., Morgan, R. M., and Eppinger, R. H., (1997) RAID- An Investigative Tool to Study Air Bag/Upper Extremity Interactions, SAE International Congress, SAE 970399
6. Robin, S., HUMOS: HUman MOdel for Safety- A Joint Effort Towards the Development of Redefined Human-like Car-occupant Models. Proc. 17th International Technical Conference on the Enhanced Safety of Vehicles, paper 297
7. van Rooij, L., Bours, R., van Hoof, J., Mihm, J. J., Ridella, S. A., Bass, C. R., Crandall, J. R., (2003) The Development, Validation and Application of a Finite Element Upper Extremity Model Subjected to Air Bag Loading, Proc. 47th Stapp Car Crash Conference, Society of Automotive Engineers, Warrendale, PA.

CONTACT

ADDITIONAL SOURCES

DEFINITIONS, ACRONYMS, ABBREVIATIONS

APPENDIX